Hematopoietic stem cell transplantation in a patient with proteasome-associated autoinflammatory syndrome (PRAAS)

Verhoeven, D.; Schonenberg-Meinema, D.; Ebstein, F.; Papendorf, J.J.; Baars, P.A.; Leeuwen, E.M.M. van; ... ; Kuijpers, T.W.

Brief report

Hematopoietic stem cell transplantation in a patient with proteasome-associated autoinflammatory syndrome (PRAAS)

Dorit Verhoeven, MD,[a,b] Dieneke Schonenberg-Meinema, MD,[a] Frédéric Ebstein, PhD,[c] Jonas J. Papendorf, MSc,[c] Paul A. Baars, PhD,[b] Ester M. M. van Leeuwen, PhD,[b] Machiel H. Jansen, BSc,[b] Arjan C. Lankester, MD, PhD,[d] Mirjam van der Burg, PhD,[e] Sandrine Florquin, MD, PhD,[f] Saskia M. Maas, MD,[g] Silvana van Koningsbruggen, PhD,[g] Elke Krüger, PhD,[c] J. Merlijn van den Berg, MD, PhD,[a] and Taco W. Kuijpers, MD, PhD[a,b] *Amsterdam and Leiden, The Netherlands; and Greifswald, Germany*

GRAPHICAL ABSTRACT

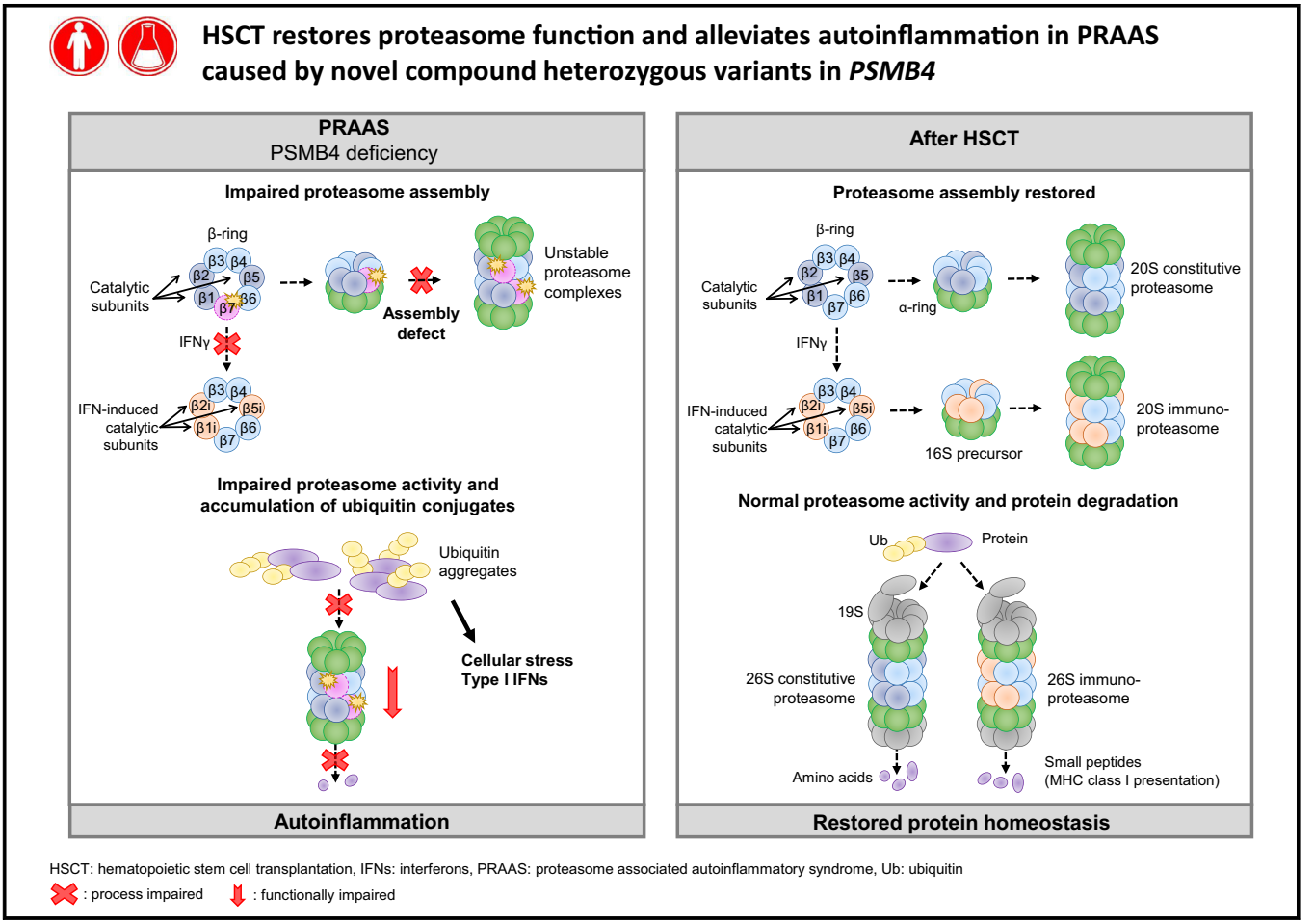

From [a]the Department of Pediatric Immunology, Rheumatology and Infectious Diseases, Emma Children's Hospital, [b]the Department of Experimental Immunology, Amsterdam Institute for Infection and Immunity, [f]the Department of Pathology, and [g]the Department of Clinical Genetics, Amsterdam University Medical Center, University of Amsterdam; [c]the Institut für Medizinische Biochemie und Molekularbiologie, Universitätsmedizin Greifswald; and [d]the Department of Pediatrics, Pediatric Stem Cell Transplantation Program, and [e]the Department of Pediatrics, Laboratory for Pediatric Immunology, Willem-Alexander Children's Hospital, Leiden University Medical Center, Leiden University.

Supported by the German Research Foundation (grant SFB-TR167 A04 [to E.K.]).
Disclosure of potential conflict of interest: The authors declare that they have no relevant conflicts of interest.

Received for publication March 16, 2021; revised July 7, 2021; accepted for publication July 28, 2021.
Available online August 17, 2021.
Corresponding author: Taco W. Kuijpers, MD, PhD, Meibergdreef 9, 1105 AZ, Amsterdam, The Netherlands. E-mail: t.w.kuijpers@amsterdamumc.nl.
The CrossMark symbol notifies online readers when updates have been made to the article such as errata or minor corrections
0091-6749

https://doi.org/10.1016/j.jaci.2021.07.039

Background: Proteasome-associated autoinflammatory syndromes (PRAASs) form a family of recently described rare autosomal recessive disorders of disturbed proteasome assembly and proteolytic activity caused by mutations in genes coding for proteasome subunits. The treatment options for these proteasome disorders consist of lifelong immunosuppressive drugs or Janus kinase inhibitors, which may have partial efficacy and noticeable side effects. Because proteasomes are ubiquitously expressed, it is unknown whether hematopoietic stem cell transplantation (HSCT) may be a sufficient treatment option.

Objective: Our aim was to report the case of a young boy with a treatment-resistant cutaneous vasculitis that was initially suspected to be associated with a gene variant in *SH2D1A*.

Methods: Whole-exome sequencing was performed to identify the genetic defect. Molecular and functional analyses were performed to assess the impact of variants on proteasomal function. The immune characterization led to the decision to perform HSCT on our patient and conduct follow-up over the 7-year period after the transplant. Because loss of myeloid chimerism after the first HSCT was associated with relapse of autoinflammation, a second HSCT was performed.

Results: After the successful second HSCT, the patient developed mild symptoms of lipodystrophy, which raised the suspicion of a PRAAS. Genetic analysis revealed 2 novel heterozygous variants in *PSMB4* (encoding proteasomal subunit β7). Retrospective analysis of patient cells stored before the first HSCT and patient cells obtained after the second HSCT demonstrated that HSCT successfully rescued proteasome function, restored protein homeostasis, and resolved the interferon-stimulated gene signature. Furthermore, successful HSCT alleviated the autoinflammatory manifestations in our patient.

Conclusion: Patients with treatment-resistant PRAAS can be cured by HSCT. (J Allergy Clin Immunol 2022;149:1120-7.)

Key words: *Autoinflammation, autoinflammatory syndrome, interferon, immunoproteasome, HSCT, PRAAS, proteasome, PSMB4*

Abbreviations used

CANDLE: Chronic atypical neutrophilic dermatosis with lipodystrophy and elevated temperature
HSCT: Hematopoietic stem cell transplantation
ISG: Interferon-stimulated gene
POMP: Proteasome maturation protein
PRAAS: Proteasome-associated autoinflammatory syndrome
PRAID: POMP-related autoinflammation and immune dysregulation disease
XLP1: X-linked lymphoproliferative disease

INTRODUCTION

Proteasome-associated autoinflammatory syndrome (PRAAS) represents any autoinflammatory disease that is characterized by multisystem inflammation caused by genomic alterations in various proteasome subunits.[1-4] Different types of PRAASs are known to date, encompassing CANDLE syndrome, which was first described in 2010 as an acronym for term *chronic atypical neutrophilic dermatosis with lipodystrophy and elevated temperature*.[5]

The underlying pathophysiology is caused by a defective ubiquitin-proteasome system that leads to diminished intracellular protein degradation and hampers removal of misfolded proteins.[6,7] The 20S proteasome core particle comprises 2 α-rings and 2 β-rings in a similar albeit mirrored α1 to α7 and β1 to β7 configuration. It contains 3 proteolytically active sites, with caspase-like, trypsin-like, and chymotrypsin-like activity, respectively. The 20S-core complex can be capped with regulatory 19S particles, forming 26S proteasomes.[7]

Since the initial finding of causative mutations in *PSMB8*, which encodes an alternative inducible catalytic proteasome subunit, namely, β5i (with the *i* standing for *immuno*; LMP7) in CANDLE (PRAAS1),[1,2] additional genes encoding components of the proteasome system have been identified to cause PRAAS-like disease.[4,8] Most frequently, patients are homozygous or compound heterozygous for *PSMB8* mutations, but other patients are compound heterozygous or heterozygous for combinations of subunits. In the latter situation, a digenic inheritance is causing additive proteasome defects.[4]

Interferon-inducible subunits can be integrated into the proteasome complex *de novo*; hence, it is called the immunoproteasome to account for increased demand of proteolytic activity in the cell.[9] Chaperone proteins help the assembly of (immuno)proteasomes, one of which is the proteasome maturation protein (POMP), causing POMP-related autoinflammation and immune dysregulation disease (PRAID [or PRAAS2]), which is clinically defined by early-onset combined immunodeficiency, inflammatory neutrophilic dermatosis, and autoimmunity.[10]

In hematopoietic cells, these immunoproteasomes are constitutively expressed.[6,11] After protein degradation, the resulting small peptides can be easily removed or enter the endoplasmic reticulum to be presented by means of the HLA class I molecules on the cell surface.[12] Because proteasome function is involved in antigen presentation both in immune cells and in the thymus, it is expected that a defect in thymoproteasome activity would impair positive antigen selection during thymic development and could therefore lead to impaired T-cell diversity. This impaired T-cell diversity could in turn be involved in autoimmunity, autoinflammation, or increased susceptibility to infection.

Interestingly, most patients with PRAAS experience autoinflammation more than a lack of immune competence. This is explained by the continuous (immuno)proteasome dysfunction causing sustained hypersecretion of type 1 interferons. Accumulation of ubiquitinated waste proteins causes cellular stress, which in turn stimulates type 1 interferon production, thus forming a vicious circle.[13,14] In patients with PRAAS, triggers such as cold, physical stress, or infections cause interferon hypersecretion, provoking inflammatory attacks that can occur in any organ.[9] Janus kinase inhibitors are used to treat PRAAS, suppressing many but not all of its manifestations and thus being ineffective in some cases.[15] With proteasomes being ubiquitously expressed, whether hematopoietic stem cell transplantation (HSCT) may rescue patients with PRAAS from persistent disease has remained unclear.

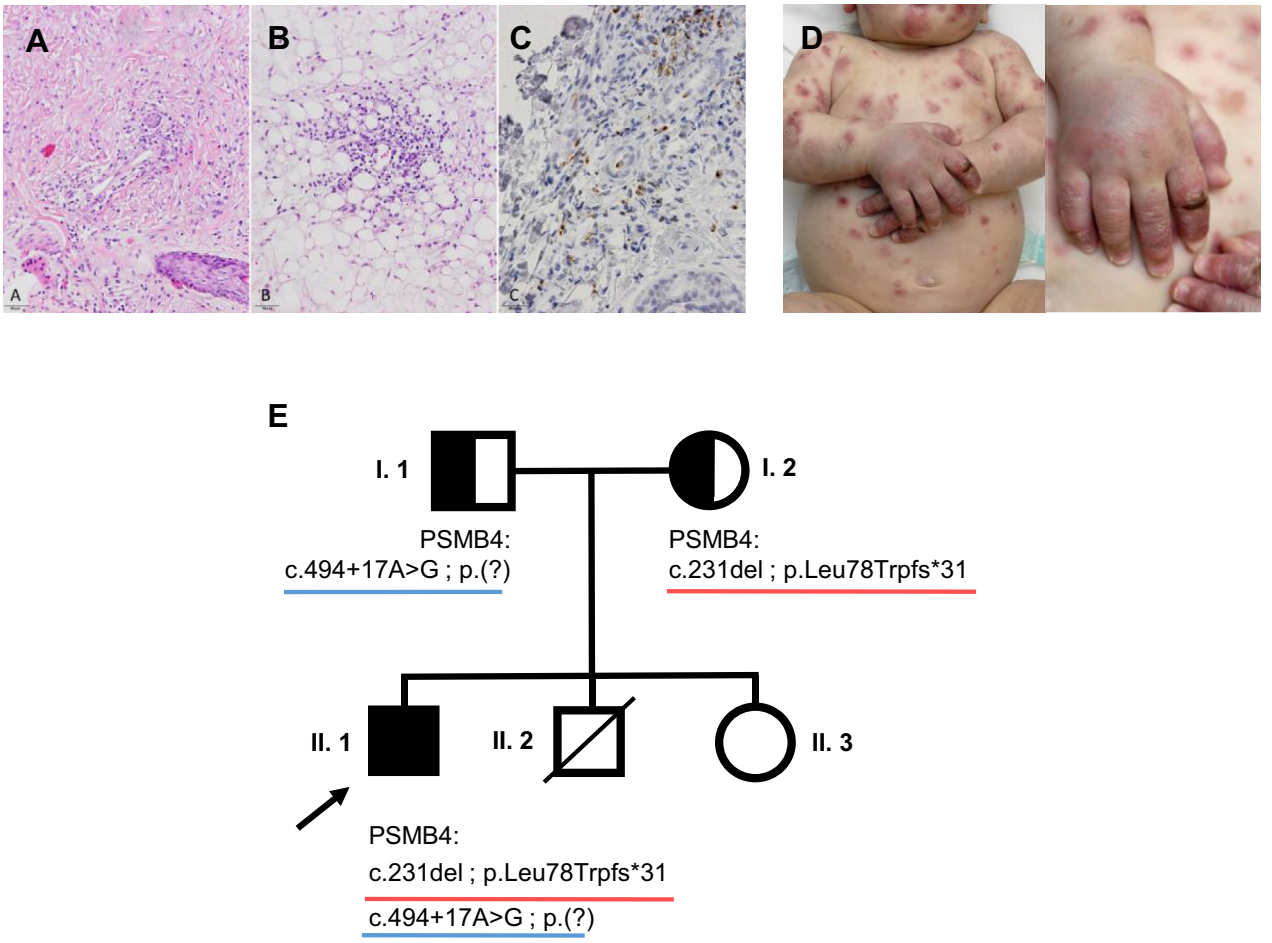

FIG 1. Clinical presentation before HSCT. **A** and **B,** Hematoxylin and eosin staining (original magnification, ×20) of the skin biopsy specimens showed superficial perivascular and interstitial inflammatory infiltrates predominantly composed of neutrophils and granulocytes intermingled with mononuclear myeloid cells. There was prominent leukocytoclasis, and some extravasation of erythrocytes was present (**A**). There was extension of the inflammation in the subcutaneous fatty tissue (**B**). **C,** Immunostaining (original magnification,×40) for granzyme B showed enrichment of granzyme B–positive cells in the inflammatory infiltrate. **D,** Pictures taken when the patient was 8 months old showing diffuse cutaneous vasculitis on the upper body and face. **E,** Family pedigree of the index patient (II.1) is indicated with an arrow; underlines in red and blue indicate maternal and paternal inheritance of mutant allele in the *PSMB4* gene, respectively. Circles represent females, squares represent males, and forward slash indicates deceased.

For detailed methods, please see the Methods section in this article's Online Repository at www.jacionline.org.

RESULTS AND DISCUSSION

In our case, a genetic diagnosis was made in hindsight in the case of a 9-year-old boy who presented at 2 months of age with skin manifestations, febrile episodes, and minor organ involvement as evidenced by chronic inflammation and slight hepatomegaly. He presented with diffuse cutaneous vasculitis (as confirmed by pathology [Fig 1, *A-D*]), which responded well to corticosteroids. On the basis of our current knowledge, he harbored 2 novel compound heterozygous mutations in *PSMB4*, encoding the constitutive β7 subunit of the proteasome,[3] which was at the time of presentation not yet known as a PRAAS gene (Fig 1, *E*). The patient was born to nonconsanguineous Dutch parents and had 2 siblings. One brother, born at 27 weeks of pregnancy, died after 2 days as a result of lung hypoplasia. All of the patient's living relatives were asymptomatic. Routine laboratory examinations showed normocytic anemia, thrombocytopenia, and increased levels of lactate dehydrogenase (see Table E1 in the Online Repository at www.jacionline.org). He tested positive for antiphospholipid autoantibodies but had no antinuclear autoantibodies. Immunophenotyping revealed abnormally high CD4/CD8 ratios owing to particularly low $CD8^+$ T-cell counts (Fig 2, *A* and *B*[16]) and an abnormal T-cell subset distribution with low percentages of naive $CD8^+$ T cells (see Fig E1, *A* in the Online Repository at www.jacionline.org). Apart from recurrent fever and vasculitis, he showed waxing and waning ferritin, lactate dehydrogenase, and aspartate aminotransferase levels with chronic thrombocytopenia, becoming therapy resistant over time despite multiple therapeutic approaches (Fig 2, *C*).

A genetic splice variant was identified by sequencing in *SH2D1A* (NM_002351.4) (c.346 +3A>G). Although the patient was EBV-negative, X-linked lymphoproliferative disease (XLP1) was considered a potential cause of his vasculitis[17];

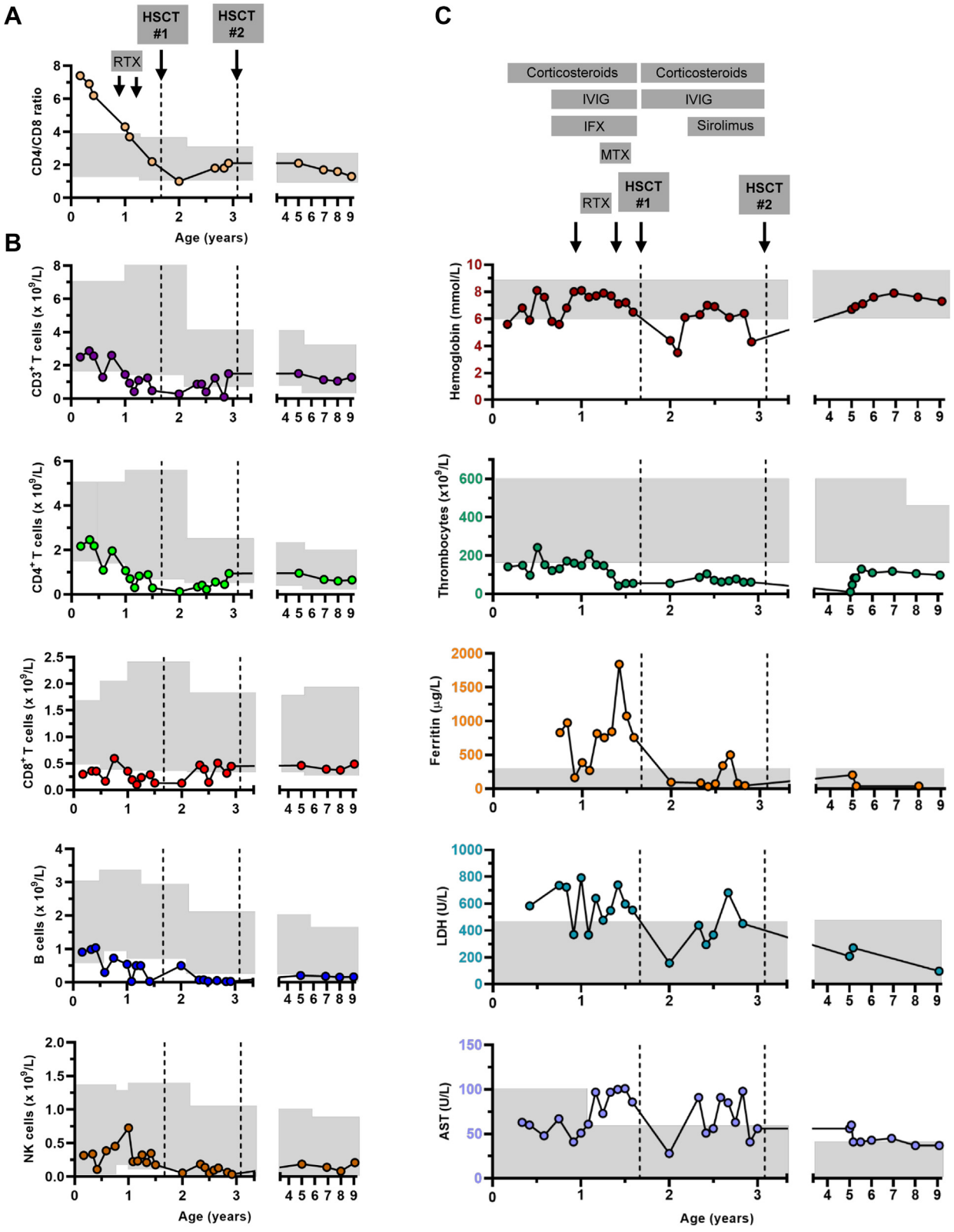

FIG 2. Clinical responses to treatment and long term follow-up. **A,** CD4/CD8 ratio before and after HSCT. The dotted lines indicate HSCT. Gray indicates age-dependent normal values.[16] **B,** Absolute numbers of $CD3^+$, $CD4^+$, and $CD8^+$ T cells, as well as B cells and natural killer (NK) cells over time.[16] **C,** Time line of the immunosuppressive therapies and levels of hemoglobin, thrombocytes, ferritin, lactate dehydrogenase (LDH), and aspartate transaminase (AST) before and after HSCTs. The dotted lines indicate HSCT. Gray indicates age-dependent reference values. *IFX*, Infliximab; *IVIG*, intravenous immunoglobulin; *MTX*, methotrexate; *RTX*, rituximab.

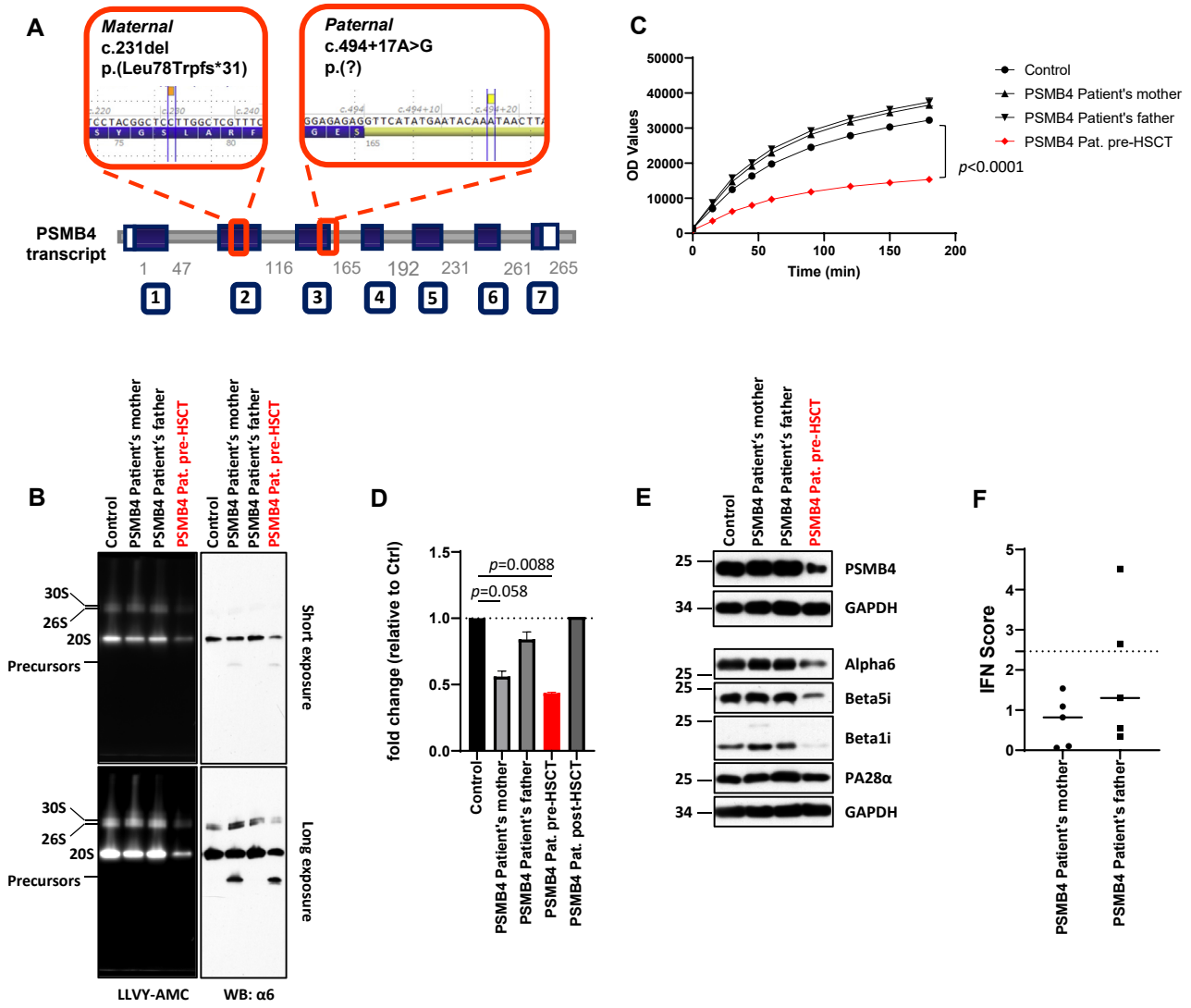

FIG 3. T cells isolated from the parents of our patient carrying both *PSMB4* variants, who are carrying either of the c.231del and c.494+17A>G genomic alterations, are devoid of proteasome defects. **A,** Schematic overview of the PSMB4 transcript of the patient illustrating the positions of the novel variants c.231del and c.494+17A>G. **B,** Whole-cell lysates from T lymphocytes isolated from the control (Ctrl), the patient (before HSCT), and his parents were separated by using 3% to 12% native-PAGE, with proteasome bands being detected by their capacity to hydrolyze the LLVY-AMC fluorogenic peptide (*left panel*). Subsequent Western blotting (WB) using an antibody specific for the α6 proteasome subunit (*right panel*) allowed the detection of 30S, 26S, and 20S mature proteasome complexes as well as proteasome precursor complexes, as indicated. **C,** The whole-cell lysates were assessed for their ability to cleave the LLVY-AMC peptide. Statistical analysis was performed with 2-way ANOVA followed by the Dunnett test. **D,** Total RNA isolated from T lymphocytes isolated from the Ctrl, the patient (before HSCT), and his parents were analyzed for PSMB4 expression by quantitative RT-PCR. Statistical analysis was performed by using the paired ratio *t* test. **E,** The whole-cell lysates were separated by SDS-PAGE and subsequently subjected to WB using antibodies specific for PSMB4/β7, α6, β5i, β1i, PA28α and glyceraldehyde-3-phosphate dehydrogenase (GAPDH) (loading Ctrl), as indicated. **F,** Gene expression of 5 typical ISGs (*IFIT1, IFI27, IFI44, ISG15,* and *RSAD2*) was assayed by quantitative RT-PCR on T cells derived from the patient's parents. Expression levels were normalized to GAPDH, and relative quantifications are presented as fold change over a calibration Ctrl, as indicated. *IFN,* Interferon.

however, the encoded protein SAP showed normal expression. HSCT was considered because of relentless severe inflammatory disease, including failure to thrive and severe growth defect, as iatrogenic damage due to chronic immunosuppression (see Table E2 in the Online Repository at www.jacionline.org). The patient's first HSCT in 2013 (at 20 months of age) with reduced intensity conditioning was followed by declining donor chimerism in the myeloid but not the lymphoid lineages and concomitant recurrence of disease manifestations (see Table E2). A year later (when the patient was 3 years old), a second HSCT with myeloablative conditioning resulted in successful grafting and persistent full donor chimerism. After 6 months of various post-HSCT infectious and HSCT-associated manifestations, most of the patient's symptoms had disappeared. During

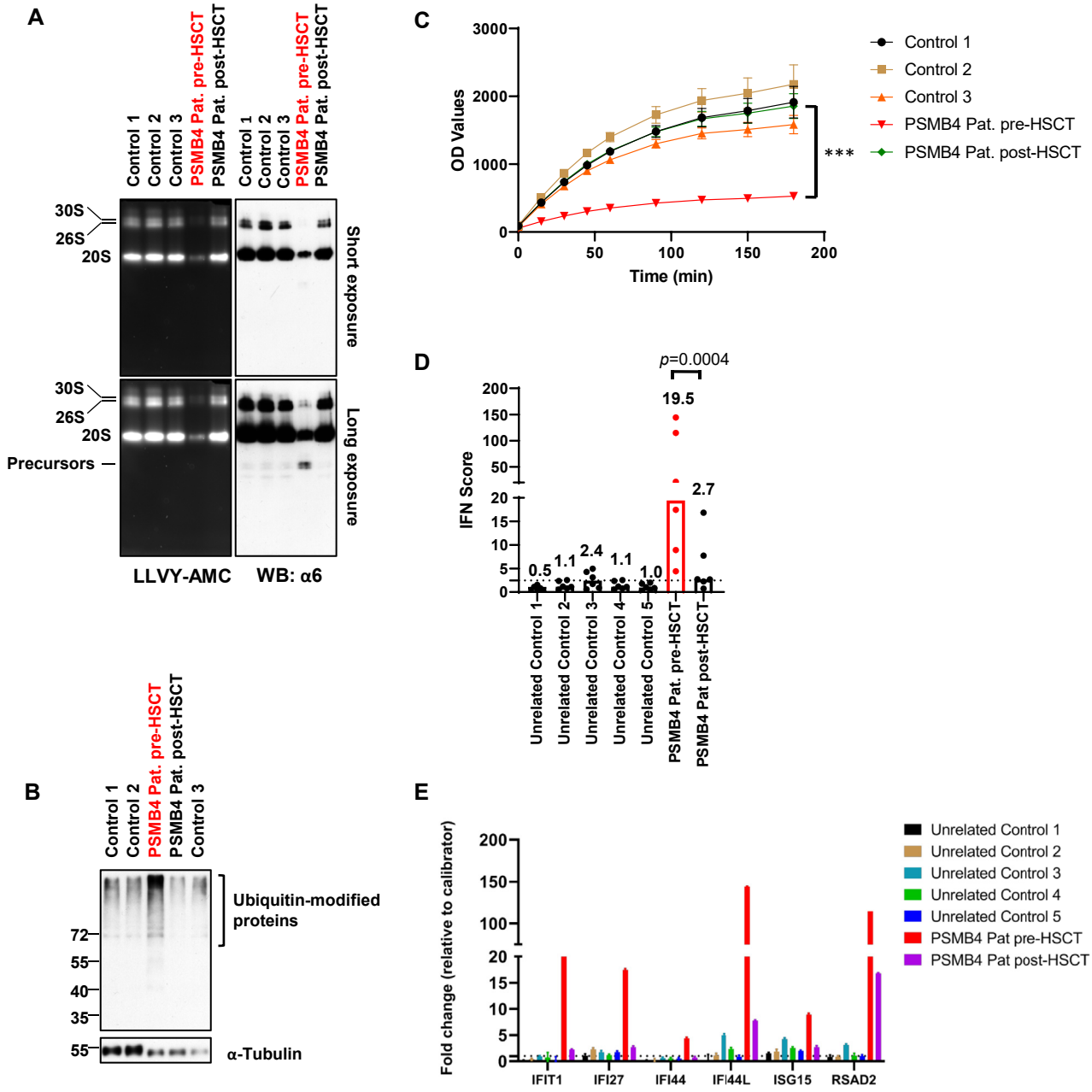

FIG 4. T cells derived from the patient carrying *PSMB4* variants exhibit reduced proteasome assembly, accumulation of ubiquitin aggregates, and an increased ISG score. **A,** Assessment of chymotrypsin-like activity in the control and patient T cells obtained at presentation and 5 years after the second HSCT by using in-gel overlay assays, with proteasome bands (30S, 26S, and 20S) being visualized by their capacity to hydrolyze the LLVY-AMC peptide (*left panel*). Native-PAGE gels were subsequently assessed for their amounts of the α6 proteasome subunit by Western blotting (WB), as indicated (*right panel*). **B,** Radioimmunoprecipitation assay cell lysates from the control and patient (before and after HSCT) T cells were separated on 10% SDS-PAGE followed by immunoblotting for ubiquitin and α-tubulin (loading control). **C,** TSDG cell lysates from the control and patient (before and after HSCT) T cells were assessed for their ability to cleave the LLVY-AMC peptide, as indicated. Statistical significance was assessed by a ratio paired *t* test (*PSMB4* of the patient [Pat.] before HSCT vs *PSMB4* of the Pat. after HSCT, ***$P < .0001$). **D,** ISG scores determined for the control and patient (before and after HSCT) T cells from the median fold change values of 6 ISGs (ie, *IFIT1*, *IFI27*, *IFI44*, *IFI44L*, *ISG15,* and *RSAD2*) over a single calibrator control by quantitative RT-PCR. Statistical significance was assessed by using the ratio paired *t* test (*PSMB4* of the Pat. before HSCT vs *PSMB4* of the Pat. after HSCT [$P = .0004$]). **E,** Gene expression of 6 typical ISGs (*IFIT1, IFI27, IFI44, IFI44L, ISG15,* and *RSAD2*) in the controls and patient (before and after HSCT). Expression levels were normalized to glyceraldehyde-3-phosphate dehydrogenase (GAPDH), and relative quantifications are presented as fold change over a calibration control, as indicated.

7 years of follow-up, his T-cell subset distribution and clinical parameters normalized apart from a persistent thrombocytopenia of around 120 × 10^9 platelets/L (Fig 2, *A-C* and see Fig E1, *B* and Table E1). Without any medication, mild signs of lipodystrophy had become clinically apparent after HSCT, at which time the patient was in poor condition and experienced cachexia too. These features remained over time and raised suspicion of lipodystrophy, although engraftment after the second HSCT was successful and catch-up growth became evident.

Because of doubt about the initial genetic diagnosis, trio-based (involving the patient and his parents) whole-exome sequencing was performed, demonstrating novel compound heterozygous and likely pathogenic variants in *PSMB4* (NM_002796.2) c.231del p.(Leu78Trpfs*31) and c.494+17A>G p.(?) (Fig 3, *A*). The first variant (which was absent from >215,000 alleles in the gnomAD cohort) was predicted to be pathogenic according to *in silico* bioinformatics tools by virtue of its causing a frameshift and creating a new stop codon, potentially causing a dysfunctional or truncated protein. This c.231del transcript variant was not detectable in the patient's T cells, suggesting that it is subjected to nonsense-mediated mRNA decay. Investigations of the mother's T cells with the single c.231del alteration showed accumulation of proteasome precursor complexes without loss of proteasome activity (Fig 3, *B* and *C*) and revealed a reduction of about 40% of PSMB4/β7 mRNA levels (Fig 3, *D*). However, the decreased amounts of PSMB4/β7 transcripts in these cells was not followed by a parallel drop in level of the PSMB4/β7 protein (Fig 3, *E*), suggesting the existence of compensatory mechanisms that increase PSMB4/β7 half-life and preserve proteasome function. *In silico* analysis of the c.494+17A>G variant, which was found 12 times in the reference gnomAD cohort, showed reduction in the strength of splicing at the splice donor site and in parallel creation of a new cryptic splice donor site, potentially causing a frameshift during translation (see Fig E2 in the Online Repository at www.jacionline.org). Analysis of the patient's T cells revealed that the c.494+17A>G alteration yields a splice variant transcript devoid of exon 4 (see Fig E3 in the Online Repository at www.jacionline.org), which has no significant impact on PSMB4/β7 expression, as determined by quantitative PCR and Western blotting in the father's T cells (Fig 3, *D* and *E*).

Thus, T cells isolated from the patient's parents carrying either of the 2 variants showed no substantial signs of proteasome dysfunction, as evidenced by unchanged levels of proteasome complexes, proteasome activity, proteasome subunit expression, and absence of positive type 1 interferon-stimulated gene (ISG) score (Fig 3, *B-F*). In contrast, subsequent functional testing of stored patient T cells obtained at presentation clearly indicated the functional relevance of the combination of these variants, as evidenced by the strong reduction of proteasome amounts and activity with parallel accumulation of ubiquitin conjugates (Fig 4, *A-C*), as well as by a significant increased ISG score (Fig 4, *D* and *E*). The patient's T cells obtained 5 years after the second HSCT clearly showed normal proteasome assembly and function and normalized ubiquitin conjugates and ISG scores. Retrospect analysis of the patient's sera for IL-6 and IL-18 levels, the latter of which is associated with autoinflammatory diseases and increased ISG scores,[4,18] showed increased levels at presentation and during graft failure, which decreased after the second (successful) HSCT (see Fig E4 in the Online Repository at www.jacionline.org). To date, only 1 other patient with compound heterozygous *PSMB4* variants has been reported to have impaired proteasome assembly and proteolytic defects (also designated PRAAS3).[4]

PRAAS should be considered in patients with early-onset systemic autoinflammation with prominent skin manifestations. Skin lesions are the first clinical sign to appear in PRAAS, and they are often present throughout the disease course. The cutaneous infiltrates in PRAAS show regulatory T cells, plasmacytoid dendritic cells, and immature granulocytes,[14] the latter 2 of which are known for their production of type 1 interferon.[19,20] The recurrence of autoinflammation and cutaneous vasculitis in our patient after the first HSCT despite lymphoid engraftment indicates the importance of myeloid cells in the pathophysiology of PRAAS-associated skin lesions.

Lipodystrophy usually starts before puberty, with disabling joint manifestations in the long term in some cases that are often absent in autosomal dominant PRAID.[21] Torrelo et al postulated different mechanisms to explain the lipodystrophy in PRAASs.[9] On the one hand, lipophagia can be the result of the proinflammatory state of adipose tissue macrophages.[22,23] Alternatively, high interferon levels may be toxic to adipocytes, as suggested by the evident lipoatrophy in patients after intramuscular IFN-β treatment.[24] This hypothesis is supported by the recent finding that a patient with a pathogenic variant in *PSMG2* (PRAAS4) showed halted lipodystrophy after treatment with the Janus kinase inhibitor ruxolitinib.[8] Furthermore, a study using small interfering RNA downregulation of PSMB8 showed that PSMB8-mediated proteasome activity is required for adipocyte differentiation *in vitro* and *in vivo*.[2] Data on PSMB4 in adipocyte differentiation are not available. Although we cannot exclude a slow worsening of the lipodystrophy in our patient, it has remained stable over the past several years. Further investigation will increase our understanding of the molecular mechanisms of lipodystrophy in patients with PRAAS.

Our case suggests that HSCT is a treatment option for the proteasome dysfunction caused by pathogenic *PSMB4* variants to alleviate PRAAS-related symptoms of autoinflammation for which chronic immunosuppressive medication is otherwise unsuccessful.

We are very grateful to the patient, his family, and the healthy donors for facilitating this work.

Clinical implications: HSCT alleviates autoinflammatory manifestations and restores proteasome function in PRAAS caused by novel compound heterozygous variants in *PSMB4*. Treatment of PRAAS by HSCT should be an option to overcome the proteasome dysfunction caused by variants in genes coding for proteasome subunits.

REFERENCES

1. Agarwal AK, Xing C, DeMartino GN, Mizrachi D, Hernandez MD, Sousa AB, et al. PSMB8 encoding the β5i proteasome subunit is mutated in joint contractures, muscle atrophy, microcytic anemia, and panniculitis-induced lipodystrophy syndrome. Am J Hum Genet 2010;87:866-72.
2. Kitamura A, Maekawa Y, Uehara H, Izumi K, Kawachi I, Nishizawa M, et al. A mutation in the immunoproteasome subunit PSMB8 causes autoinflammation and lipodystrophy in humans. J Clin Invest 2011;121:4150-60.
3. Brehm A, Krüger E. Dysfunction in protein clearance by the proteasome: impact on autoinflammatory diseases. Semin Immunopathol 2015;37:323-33.
4. Brehm A, Liu Y, Sheikh A, Marrero B, Omoyinmi E, Zhou Q, et al. Additive loss-of-function proteasome subunit mutations in CANDLE/PRAAS patients promote type I IFN production. J Clin Invest 2015;125:4196-211.

5. Torrelo A, Patel S, Colmenero I, Gurbindo D, Lendínez F, Hernández A, et al. Chronic atypical neutrophilic dermatosis with lipodystrophy and elevated temperature (CANDLE) syndrome. J Am Acad Dermatol 2010;62:489-95.
6. Seifert U, Bialy LP, Ebstein F, Bech-Otschir D, Voigt A, Schröter F, et al. Immunoproteasomes preserve protein homeostasis upon interferon-induced oxidative stress. Cell 2010;142:613-24.
7. Collins GA, Goldberg AL. The Logic of the 26S Proteasome. Cell 2017;169:792-806.
8. de Jesus AA, Brehm A, VanTries R, Pillet P, Parentelli AS, Montealegre Sanchez GA, et al. Novel proteasome assembly chaperone mutations in PSMG2/PAC2 cause the autoinflammatory interferonopathy CANDLE/PRAAS4. J Allergy Clin Immunol 2019;143:1939-43.e8.
9. Torrelo A. CANDLE syndrome as a paradigm of proteasome-related autoinflammation. Front Immunol 2017;8:927.
10. Poli MC, Ebstein F, Nicholas SK, de Guzman MM, Forbes LR, Chinn IK, et al. Heterozygous truncating variants in POMP escape nonsense-mediated decay and cause a unique immune dysregulatory syndrome. Am J Hum Genet 2018;102:1126-42.
11. Aki M, Shimbara N, Takashina M, Akiyama K, Kagawa S, Tamura T, et al. Interferon-gamma induces different subunit organizations and functional diversity of proteasomes. J Biochem 1994;115:257-69.
12. Sijts EJ, Kloetzel PM. The role of the proteasome in the generation of MHC class I ligands and immune responses. Cell Mol Life Sci 2011;68:1491-502.
13. Ebstein F, Poli Harlowe MC, Studencka-Turski M, Krüger E. Contribution of the unfolded protein response (UPR) to the pathogenesis of proteasome-associated autoinflammatory syndromes (PRAAS). Front Immunol 2019;10:2756.
14. Torrelo A, Colmenero I, Requena L, Paller AS, Ramot Y, Richard Lee CC, et al. Histologic and immunohistochemical features of the skin lesions in CANDLE syndrome. Am J Dermatopathol 2015;37:517-22.
15. Sanchez GAM, Reinhardt A, Ramsey S, Wittkowski H, Hashkes PJ, Berkun Y, et al. JAK1/2 inhibition with baricitinib in the treatment of autoinflammatory interferonopathies. J Clin Invest 2018;128:3041-52.
16. Comans-Bitter WM, de Groot R, van den Beemd R, Neijens HJ, Hop WC, Groeneveld K, et al. Immunophenotyping of blood lymphocytes in childhood. Reference values for lymphocyte subpopulations. J Pediatr 1997;130:388-93.
17. Booth C, Gilmour KC, Veys P, Gennery AR, Slatter MA, Chapel H, et al. X-linked lymphoproliferative disease due to SAP/SH2D1A deficiency: a multicenter study on the manifestations, management and outcome of the disease. Blood 2011;117:53-62.
18. Weiss ES, Girard-Guyonvarc'h C, Holzinger D, de Jesus AA, Tariq Z, Picarsic J, et al. Interleukin-18 diagnostically distinguishes and pathogenically promotes human and murine macrophage activation syndrome. Blood 2018;131(13):1442-55.
19. Mostafavi S, Yoshida H, Moodley D, LeBoité H, Rothamel K, Raj T, et al. Parsing the interferon transcriptional network and its disease associations. Cell 2016;164:564-78.
20. Jegalian AG, Facchetti F, Jaffe ES. Plasmacytoid dendritic cells: physiologic roles and pathologic states. Adv Anat Pathol 2009;16:392-404.
21. McDermott A, Jacks J, Kessler M, Emanuel PD, Gao L. Proteasome-associated autoinflammatory syndromes: advances in pathogeneses, clinical presentations, diagnosis, and management. Int J Dermatol 2015;54:121-9.
22. Torrelo A, Noguera-Morel L, Hernández-Martín A, Clemente D, Barja JM, Buzón L, et al. Recurrent lipoatrophic panniculitis of children. J Eur Acad Dermatol Venereol 2017;31:536-43.
23. Hill DA, Lim HW, Kim YH, Ho WY, Foong YH, Nelson VL, et al. Distinct macrophage populations direct inflammatory versus physiological changes in adipose tissue. Proc Natl Acad Sci U S A 2018;115(22):E5096-105.
24. Weise G, Hupp M, Kerstan A, Buttmann M. Lobular panniculitis and lipoatrophy of the thighs with interferon-ß1a for intramuscular injection in a patient with multiple sclerosis. J Clin Neurosci 2012;19:1312-3.

METHODS

Patient and treatment approach

The patient was hospitalized at Emma Children's Hospital in Amsterdam, The Netherlands, where he received treatment according to established clinical guidelines. All blood samples used for immunobiologic analyses were obtained after informed consent (National PID Study NL40331.078). PBMCs were isolated by density centrifugation over Ficoll-Paque media according to the standard procedures.[E1]

Conditioning regimens for HSCTs

The first HSCT was performed in February 2013 with a 10/10 matched unrelated donor after a conditioning regimen consisting of treosulfan, fludarabine, and antithymocyte globulin. The patient received cyclosporine and methotrexate as graft-versus-host disease prophylaxis. The post-HSCT course was complicated by persistent autoinflammation, skin vasculitis, and development of an ileus that was possibly triggered by intestinal viral infections. Initially, the patient attained greater than 95% donor chimerism in the PBMC and granulocyte lineages; however, a decline in donor chimerism became apparent after 3 months. Lineage studies conducted after 4 and 7 months showed donor chimerism of 95% to 100% in $CD4^+$ and $CD8^+$ T-cell populations, 80% to 90% in natural killer (NK) cells, and less than 30% in the $CD14^+CD33^+$ myeloid lineage. Because of almost complete donor chimerism in his T-cell and NK cell compartments, this suggested that the clinical relapse of autoinflammation was caused by residual autologous cells other than the T or NK cells. Five months after transplantation the patient was treated with an intravenous infusion of autologous $CD34^+$ peripheral blood stem cells from the same unrelated donor, which had no effect. The second HSCT was performed in June 2014 with the same donor after conditioning with busulfan, fludarabine, and alemtuzumab. The patient received cyclosporine and methotrexate as graft-versus-host disease prophylaxis. After the second transplantation, the patient showed 100% persistent donor chimerism.

Histology

Skin biopsy specimens were fixed in 4% formalin, embedded in paraffin, and then cut and stained with hematoxylin and eosin and analyzed using conventional light microscopy.

Immunophenotyping

Absolute numbers of thrombocytes and ferritin levels were routinely measured according to the established diagnostic guidelines. Absolute numbers of lymphocytes were determined with Multitest 6-color reagents (BD Biosciences, San Jose, Calif) according to the manufacturer's instructions. For additional flow cytometry, PBMCs were resuspended in PBS containing 0.5% (wt/vol) BSA and 0.01% sodium azide and then incubated with saturating concentrations of fluorescently labeled conjugated mAb antibodies. Patient samples were analyzed simultaneously with PBMCs from healthy donors. The following directly conjugated mAbs were used: CD3-APC, CD3–APC-H7, CD4–PE-Cy7, CD4-PerCP-Cy5.5, CD8-PerCP-Cy5.5, CD19-PerCP-Cy5.5, CD20-APC, and CD56-FITC (from BD Biosciences); IgD-PE and gamma-1 isotype (from BD Pharmingen, San Diego, Calif); CD20-APC (from Biolegend San Diego, Calif); CD16-FITC and CD27-FITC (from Sanquin, Amsterdam, The Netherlands); and CD45RA-PE (RD-1) (from Beckman Coulter, Brea, Calif). Analysis of cells was performed using a FACS Calibur or Canto-II flow cytometer (from BD Biosciences) and FlowJo software.

Clinical parameters and cytokine measurements

The hemoglobin, thrombocytes, lactate dehydrogenase, aspartate transaminase, and ferritin levels and additional parameters provided in Table E1 were derived from clinical measurements. IL-18 and IL-6 levels were measured in 50 μL of plasma or serum by multiplex technology as described previously (xMAP, Luminex, Austin, Tex).[E2]

Sequencing

Whole-exome capture and sequencing were performed using SeqCap EZ MedExome (Roche NimbleGen, Pleasanton, Calif). The resulting libraries were sequenced on a HiSeq4000 sequencer (Illumina, San Diego, Calif) according to the manufacturer's recommendations for paired-end 150-bp reads. Alignment of sequence reads to human reference genome (hg19) was done by using BWAMEM 0.7.10 (bio-bwa.sourceforge.net/), and variants were called by using the GATK3.3 software package (www.broadinstitute.org/gatk/). Filtering of variants was done by using Alissa Interpret (Agilent Technologies, Santa Clara, Calif). Variants with fewer than 5 reads and a frequency of more than 1% in public (ESP, dbSNP, and 1KG) and/or in-house databases were excluded. *De novo*, homozygous, or compound heterozygous variants present in exons or within plus or minus 6 nt in the intron were evaluated.

Splice site variants

Alamut software (www.interactive-biosoftware.com/doc/alamut-visual/2.6/splicing.html) was used to analyze possible splice sites. This tool includes SpliceSiteFinder-like, MaxEntScan, NNSPLICE, and GeneSplicer.

Native PAGE, proteasome assembly, and Western blotting

PBMCs collected from healthy individuals, parents, and patients (with or without HSCT) were subjected to T-cell expansion by cultivating them together with irradiated feeder cells in the presence of IL-2 (50 U/mL) and L-PHA (1 mg/mL) for 3 to 4 weeks following the procedure of Fonteneau et al.[E3] Cell pellets from resting T cells were lysed in ice-cold homogenization TSDG buffer (10 mM Tris [pH 7.0], 10 mM NaCl, 25 mM KCl, 1.1 mM $MgCl_2$, 0.1 mM EDTA, 2 mM dithiothreitol, 2 mM ATP, 1 mM NaN_3, and 20 % glycerol), and proteins were extracted by using freezing-thawing in liquid nitrogen. Protein quantification of the soluble lysates was performed by using a standard bicinchoninic acid assay (from Thermo Fisher Scientific, Waltham, Mass). Twenty micrograms of whole-cell lysates were run on 3% to 12% gradient Bis-Tris gels (Thermo Fisher Scientific) at 45 V overnight at 4°C by using an electrophoresis buffer consisting of 50 mM BisTris and 50 mM Tricine (pH 6,8). Following separation, chymotrypsin-like proteasome peptidase activity was measured by incubating the gels with 0.1 mM of the Suc-LLVY-AMC fluorogenic peptide (Bachem) at 37°C for 20 minutes in an overlay buffer (20 mM Tris, 5 mM $MgCl_2$ [pH 7,0]). Proteasome bands were subsequently visualized by exposing the gel to UV light at 360 nm and detected at 460 nm by using a Fusion FX Imager (Vilber, Collegien, France). Gels were further blotted onto polyvinylidene difluoride membranes, which were then probed with an anti-α6 primary antibody (clone MCP20, Enzo Life Sciences, Farmingdale, NY) to monitor the amounts of proteasome complexes. Antibody binding was detected by using anti-mouse horseradish peroxidase–labeled secondary antibody and chemiluminescence (Bio-Rad, Hercules, Calif).

SDS-PAGE and Western blotting

Cell pellets from resting T cells isolated from the patient (with or without HSCT), his parents, and controls were lysed in equal amounts of standard radioimmunoprecipitation assay buffer (50 mM Tris [pH 7.5], 150 mM NaCl, 2 mM EDTA, 1 mM N-ethylmaleimide, 10 μM MG-132, 1% NP40, and 0.1% SDS) and separated by 10 % SDS-PAGE before transfer to polyvinylidene difluoride membranes (200 V for 1 hour). After blocking (a 20-minute exposure to 1× Roti-Block at room temperature), membranes were probed with antiubiquitin (clone FK2, Enzo Life Sciences), PSMB4/β7 (Abcam, ab137087), α6 (clone MCP20, Enzo Life Sciences), β5i (clone A-12, Santa Cruz Biotechnology, Dallas, Tex), β1i (K221, laboratory stock), PA28α (K232/1, laboratory stock) glyceraldehyde-3-phosphate dehydrogenase (GAPDH) (clone 14C10, Cell Signaling Technology, Danvers, Mass), and α-tubulin (clone DM1A, Abcam) primary antibodies overnight at 4°C, after which they were washed 3 times with PBS/0.2% Tween and subsequently incubated with anti-mouse–conjugated secondary antibodies (1/5.000) for 1 hour at room

temperature. Proteins were then visualized by using an enhanced chemiluminescence detection kit (Bio-Rad).

In-plate peptidase activity assay

The chymotrypsin-like activity of the T cells of the control, the patients' parents, and the patient (with or without HSCT) was assessed on black 96-well microtiter plates (Greiner, Kremsmünster, Austria) by incubating 10 μg of TSDG-generated whole-cell lysates with 0.1 mM Suc-Leu-Leu-Val-Tyr-AMC proteasome substrate in quadruplicate in a final volume of 100 μL. Free AMC release following peptide digestion was measured over a 3-hour period by using a fluorescence plate reader at 360/460 nm (NanoQuant Plate, Tecan, Männedorf, Switzerland).

RNA extraction and quantitative RT-PCR

Total RNA was isolated from resting T cells by using the kit from Analytic Jena AG (Jena, Germany) following the manufacturer's instructions. For subsequent real-time PCR, 100 to 500 ng of the isolated total RNA was reverse-transcribed by using the M-MLV reverse transcriptase (Promega, Madison, Wis). Quantitative PCR was performed by using the Premix Ex Taq (probe quantitative PCR purchased from TaKaRa, Shiga, Japan) and in duplicate to determine the mRNA levels of 6 ISGs by using FAM-tagged TaqMan Gene Expression Assays obtained from Thermo Fisher Scientific according to the manufacturer's instructions. The TaqMan probes used in this study for ISG quantification included *IFI27, IFI44L, IFIT1, ISG15, RSAD2,* and *IFI44*. The cycle threshold (Ct) values for the target genes were converted to values of relative expression by using the relative quantification method ($2^{-\Delta\Delta Ct}$). Target gene expression was calculated relative to Ct values for the GAPDH control housekeeping gene. A type 1 interferon score representing the median fold change of the 6 ISGs relative to a single calibrator control was calculated for each sample following the procedure of Rice et al.[E4]

PSMB4 sequence analysis

Full-length PSMB4 RT-PCR was performed on total RNA extracted from the index case patient's T cells, and the PCR products were subsequently cloned into the pCR 2.1-TOPO vector (Invitrogen, Waltham, Mass) according to the manufacturer's instructions. The resulting constructs were sent for sequencing (Microsynth AG, Balgach, Switzerland) using the M13 reverse primer.

Statistical analysis

The data were typically means plus or minus SEMs, and they were analyzed by pair ratio *t* test between 2 groups. All charts and statistical analyses were generated using GraphPad Prism 8. A *P* value less than .05 was considered significant. All data are available from the authors on request.

REFERENCES

E1. Kuijpers TW, van Leeuwen EM, Barendregt BH, Klarenbeek P, aan de Kerk DJ, Baars PA, et al. A reversion of an IL2RG mutation in combined immunodeficiency providing competitive advantage to the majority of CD8+ T cells. Haematologica 2013;98:1030-8.

E2. de Jager W, Prakken BJ, Bijlsma JW, Kuis W, Rijkers GT. Improved multiplex immunoassay performance in human plasma and synovial fluid following removal of interfering heterophilic antibodies. J Immunol Methods 2005;300:124-35.

E3. Fonteneau JF, Larsson M, Somersan S, Sanders C, Münz C, Kwok WW, et al. Generation of high quantities of viral and tumor-specific human CD4+ and CD8+ T-cell clones using peptide pulsed mature dendritic cells. J Immunol Methods 2001;258:111-26.

E4. Rice GI, Melki I, Frémond ML, Briggs TA, Rodero MP, Kitabayashi N, et al. Assessment of type I interferon signaling in pediatric inflammatory disease. J Clin Immunol 2017;37:123-32.

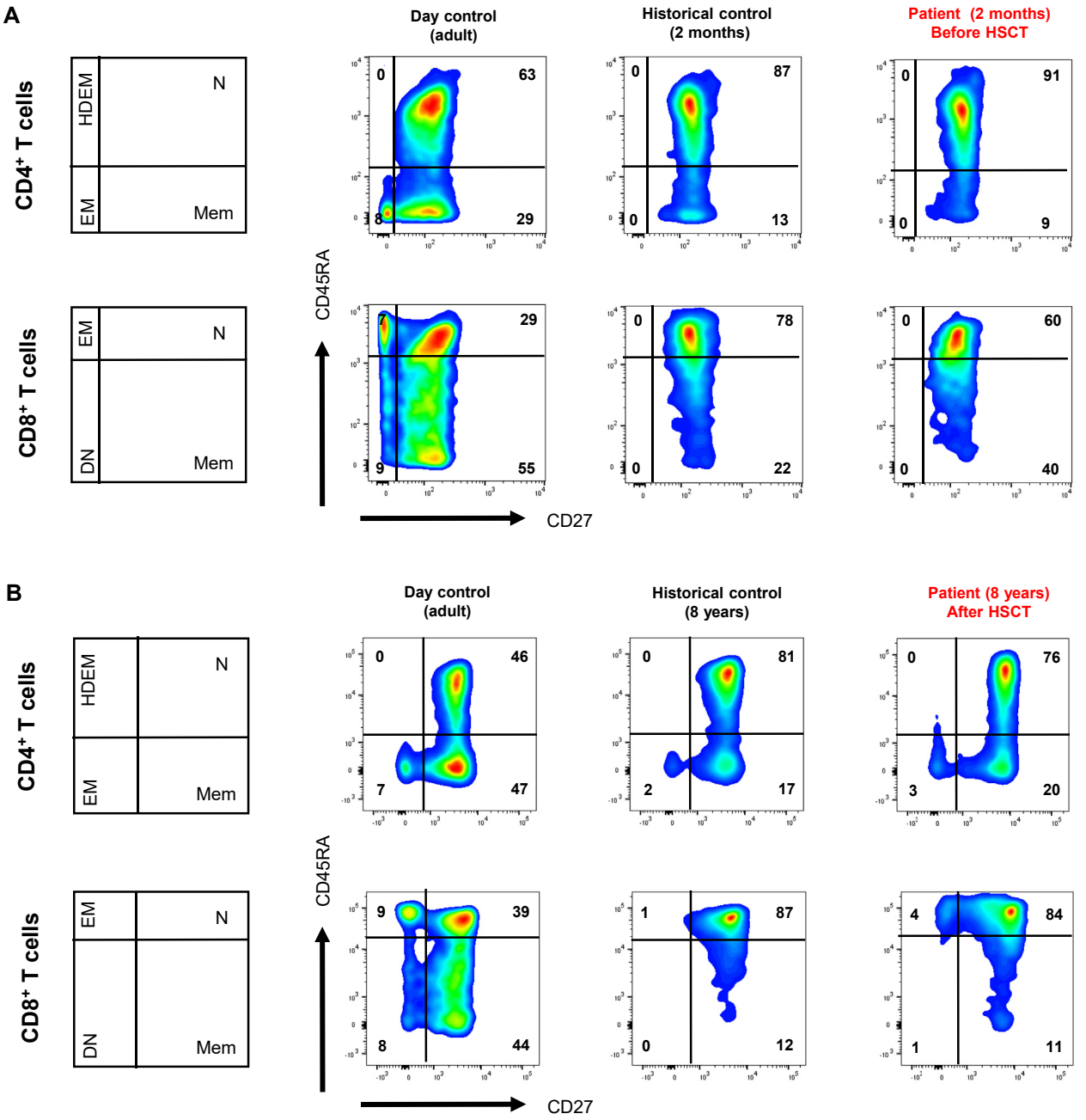

FIG E1. The patient with PSMB4-PRAAS showed a reduced number of naive $CD8^+$ T cells before HSCT. **A** and **B,** Fluorescence-activated cell sorting plots show CD27/CD45RA memory distribution of the $CD3^+CD4^+$ and $CD3^+CD8^+$ T cells of our patient at 2 months and 8 years of age. Numbers indicate percentage of naive (N), memory (Mem), effector memory (EM), highly differentiated effector memory (HDEM) ($CD4^+$), and double-negative (DN) ($CD8^+$) subpopulations. An age-matched historical control and an (adult) day control were provided to certify subset gating strategy.

A

Population	Allele Count	Allele Number	Number of Homozygotes	Allele Frequency
European (non-Finnish)	12	129092	0	0.00009296
African/African-American	0	24968	0	0.000
Latino/Admixed American	0	35428	0	0.000
Ashkenazi Jewish	0	10358	0	0.000
East Asian	0	19952	0	0.000
European (Finnish)	0	25110	0	0.000
Other	0	7220	0	0.000
South Asian	0	30616	0	0.000
Female	6	129444	0	0.00004635
Male	6	153300	0	0.00003914
Total	**12**	**282744**	**0**	**0.00004244**

B

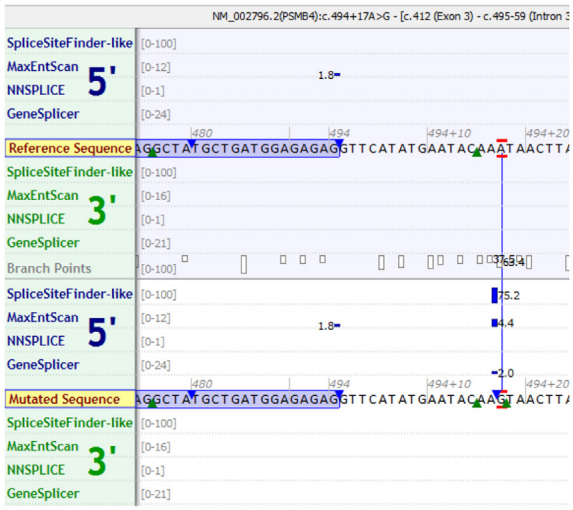

FIG E2. *In silico* analysis of the c.494+17A>G variant. **A,** Snapshot of the allele frequency of c.494+17A>G p.(?) in the gnomAD cohort. **B,** Snapshot of the *in silico* prediction scores as reported in the Alamut web tool for the c.494+17A>G p.(?) variant. The splice site scores for the original (*top section*) and new splice sites (*lower section*) are provided.

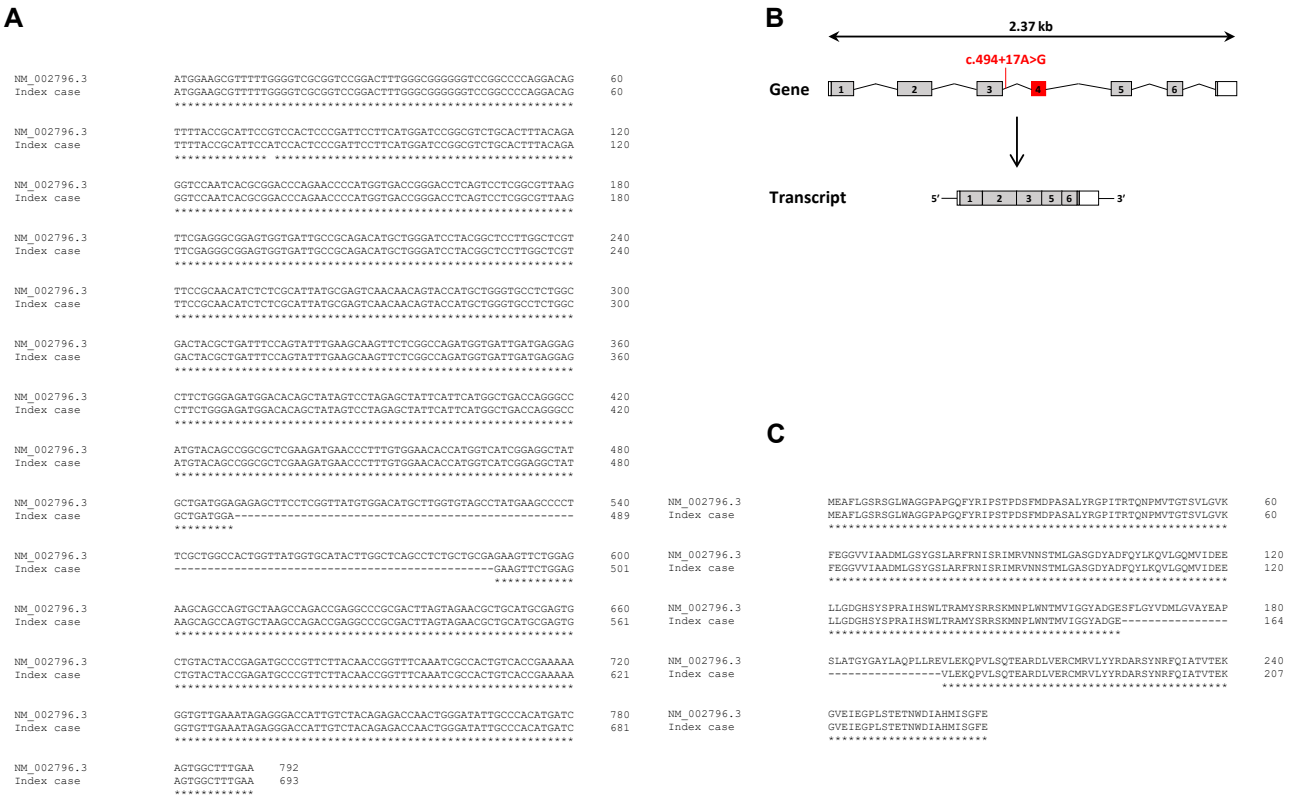

FIG E3. The c.494+17A>G alteration yields a PSMB4/β7 alternative splice variant. **A,** Alignment of *Homo sapiens* proteasome 20S subunit beta 4 (PSMB4) mRNA (NM_002796.3) and a PSMB4 cDNA species isolated from the PSMB4 index case carrying both c.231del and c.494+17A>G genomic alterations. **B,** Illustration of the generation of a PSMB4 splice variant transcript devoid of 99 nucleotides mostly corresponding to exon 4 of the PSMB4 gene (*red*). **C,** Alignment of PSMB4/β7 and PSMB4/β7(Δ165-197) proteins, with the latter representing the identified splice variant comprising an in-frame deletion of 33 amino acids, as indicated.

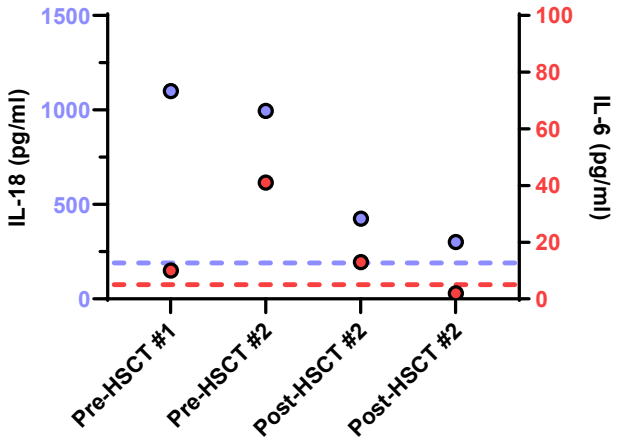

FIG E4. Decrease in IL-18 and IL-6 levels after HSCT. Cytokine Luminex assay on patients' plasma or serum samples obtained before the first HSCT, before the second HSCT, and twice after the second HSCT. Dotted lines depict laboratory reference values of healthy individuals.

TABLE E1. Routine biologic findings in the patient

Indicator	8/31/2011	10/19/2011 - 11/25/2011	3/30/2012 - 6/4/2012	HSCT No. 1	6/12/2013	HSCT No. 2	6/12/2017	7/27/2020
Age	2 mo	3-4 mo	9-11 mo		2 y		6 y	9 y
Complete blood cell count								
White blood cells (10^9/L), median (range)	**5.2*** (6.0-21.0)	6.9 (5.0-15.0)	5.9 (5.0-15.0)				4.5 (4.0-15.0)	4.0 (4.0-14.0)
Eosinophils (10^9/L), median (range)	NA	0.31 (0-0.8)	0.02 (0-0.8)		0.02 (0-0.8)		0.10 (0-0.8)	0.08 (0-0.5)
Basophils (10^9/L), median (range)	NA	0.02 (0-0.2)	0.02 (0-0.2)		0.01 (0-0.2)		0.02 (0-0.2)	0.01 (0-0.2)
Neutrophils (10^9/L), median (range)	NA	3.67 (1.0-5.0)	2.35 (1.0-5.0)		**9.35**† (1.0-8.0)		2.08 (1.5-9.0)	2.08 (1.5-8.0)
Lymphocytes (10^9/L), median (range)	NA	5.25 (4.0-10.0)	1.77 (1.5-9.5)		**0.55*** (1.5-9.5)		2.06 (1.0-6.0)	1.58 (1.0-5.0)
Monocytes (10^9/L), median (range)	NA	1.00 (0.4-1.2)	0.33 (0.2-1.0)		0.56 (0.2-1.0)		0.27 (0.1-1.0)	0.26 (0.1-1.0)
Hemoglobin level (mmol/L), median (range)	**5.6*** (6.0-9.0)	6.4 (6.0-9.0)	**5.6*** (6.0-9.0)		**4.4*** (6.0-9.0)		7.6 (6.0-9.0)	7.3 (6.0-9.0)
Mean corpuscular volume (fL), median (range)	NA	NA	70 (70-84)		NA		NA	84 (75-95)
Reticulocytes (10^9/L), median (range)	NA	NA	45.80 (25-100)		NA		NA	NA
Thrombocytes counts (10^9/L), median (range)	**141*** (150-600)	**124*** (150-600)	**131*** (150-600)		**58*** (150-600)		**110*** (150-600)	**98*** (150-450)
Biochemistry								
Triglycerides (g/L), median (range)	NA	NA	NA		NA		NA	NA
C-Reactive protein level (mg/L), median (range)	NA	0.9 (<5.0)	**15.3**† (<5.0)		**8.7**† (<5.0)		0.3 (<5.0)	0.3 (<5.0)
Alkaline phosphatase level (U/L), median (range)	NA	359 (50-400)	NA		180 (50-400)		**357**† (60-325)	NA
Gamma-GT level (U/L), median (range)	NA	29 (0-56)	NA		**229**† (0-56)		21 (0-56)	NA
AST (U/L), median (range)	NA	63 (0-95)	67 (0-95)		28 (0-60)		**43**† (0-40)	37
ALT(U/L), median (range)	NA	44 (0-65)	23 (0-65)		23 (0-45)		29 (0-45)	NA
LDH (U/L), median (range)	NA	**583**† (0-466)	**736**† (0-466)		158 (0-466)		NA	NA
CPK (U/L), median (range)	NA	145 (0-250)	**343**† (0-250)		101 (0-250)		NA	NA
Ferritin (μg/L), median (range)	NA	*NA*	**830-1047**† (25-300)		96 (25-300)		NA	38 (0-40)
Immunology								
IgA (g/L)	NA	0.13 (0.12-0.7)	0.23 (0.12-0.7)		**0.04*** (0.12-0.8)		0.35 (0.12-1.6)	0.47 (0.14-2.1)
IgG (g/L)	NA	3.8 (2-12)	4.4 (2-12)		**0.6*** (2-11)		7.2 (4.1-10.6)	6.9 (4.1-12.3)
IgM (g/L)	NA	**1.14*** (0.14-0.9)	0.44 (0.14-0.9)		**0.07*** (0.09-0.7)		0.69 (0.2-1.5)	0.41 (0.11-1.3)
Autoimmunity markers	ANA/ENA neg	ANA neg, aCL-IgG pos, aB2 GPI-IgG pos	ANA neg, Coombs pos		ANA neg		ANA neg Coombs neg	ANA neg

Abnormal values are in boldface.

aCL, Anticardiolipin; *ALT,* alanine transaminase*; ANA,* antinuclear antibody*; AST*, aspartate transaminase*; CPK,* creatine phosphokinase*; ENA,* extractable nuclear antigen; *GP1*, glycoprotein 1; *Gamma-GT*, Gamma-glutamyltransferase; *LDH*, lactate dehydrogenase; *NA*, not available/applicable.

*Value lower than age-specific normal value.

†Value higher than age-specific normal value.

TABLE E2. Therapeutic strategies before HSCT

Time line	Therapy	Dosage	Clinic/symptoms
August 2011	Cutaneous corticosteroids		
October 2011-February 2012	Prednisolone Flucanozol	1 mg/kg	Vasculitis
March 2012	MP pulse i.v.	15 mg/kg	Flare vasculitis, fever, swollen and painful hands
April-July 2012	IFX IVIG Prednisone RTX (May 2012)	5 mg/kg/2 wk 2 g/kg/4 wk 2 times-a-day 5 mg 2×375 mg/m^2	Flare vasculitis
August 2012	MP pulse i.v.	25 mg/kg	
September-November 2012	IFX IVIG Prednisone	10 mg/kg/2 wk 2 g/kg/4 wk 2 times-a-day 5 mg	Flare vasculitis
December 2012-January 2013	IFX MTX RTX (December 2012)	10 mg/kg/2 wk 2.5 mg/1 wk 1×375 mg/m^2	Persistence of recurrent flare
February 2013	First HSCT (conditioning Treo, Flu, ATG)		
April-June 2013	Prednisone MSC (2x) IFX	1-2 mg/kg 10 mg/kg/2 wk	Enteral inflammation suspected of GVHD (biopsy, nonproved) Astrovirus infection
July 2013	$CD34^+$ PBSC boost		
August-December 2013	Prednisone tapering		
January 2014	IVIG Prednisone Desloratadine	2 g/kg/4 wk 2 times-a-day 5 mg 2 times-a-day 2.5 mg	Fever Persistent sapovirus
February-May 2014	IVIG Prednisone Sirolimus	2 g/kg/4 wk $\leq$2 times-a-day 5 mg 1 time-a-day 1.5 mg	
June 2014	Second HSCT (myeloid ablative conditioning: Flu, BU, Campath)		

ATG, Antithymocyte globulin; *BU*, busulfan; *Campath*, alemtuzumab; *Flu*, fludarabine; *GVHD*, graft-versus-host disease; *IFX*, infliximab; *i.v.*, intravenous; *MP*, methylprednisolone; *MSC*, mesenchymal stroma cell; *MTX*, methotrexate; *PBSC*, peripheral blood stem cell; *RTX*, rituximab (anti-CD20); *Treo*, treosulfan.